XPS, AES and EELS study of the bonding character in CN_x films

G. Soto, E.C. Sámano, R. Machorro, F.F. Castillón, M.H. Farías and L. Cota-Araiza.
Centro de Ciencias de la Materia Condensada, UNAM,
Apdo. Postal 2681, 22800 Ensenada, B. C., México.

We discuss the possibility of using photoemitted electrons corresponding to carbon 1s, in order to resolve the chemical state and the hybridization character of carbon in amorphous carbon nitride films (*a-CN$_x$*). A series of carbon nitride films were prepared at room temperature by ablating a graphite target in a background of molecular nitrogen in the pressure range from high vacuum to 500 mTorr. The films were analyzed by means of *XPS*, *EELS* and *AES*. *XPS* results show the existence of two predominant binding states for both, nitrogen and carbon. The effect of heat treatment is to decrease the nitrogen content in the films, and the sharpening of the binding configuration of carbon. *EELS* results indicate that the films have predominantly *sp^2*-hybridized carbon, before and after heat treatment, and no evidence of carbon in the *sp^3* configuration was found. Thereupon, we conclude that it is not feasible to determine the hybridization state for carbon from *XPS* measurements alone, and that the nitrogen and carbon are co-existent in a polymer-like film.

Keywords: Carbon nitride films; *XPS*; *AES*; *EELS*; Polymer; Chemical state
PACS numbers: 81.05.Je, 81.15.Fg, 81.40.Tv

1. Introduction

In the past years, a large number of scientific reports have dealt with the preparation and characterization of carbon nitride films. The impelling force of this experimental effort is the conjecture attributed to Cohen [1] that a solid formed by carbon and nitrogen would have a very high elastic bulk modulus. This prediction is based on the fact that the *C-N* bond is highly covalent with a short interatomic distance. This conjecture was tested a posteriori by several *ab initio* calculations using the kwon β-*Si$_3$N$_4$* as a prototype structure [2,3]. So far, several *CN* structures have been theoretically proposed [4] resulting in two kinds of materials. Some of them are characterized by tetrahedrally coordinated *sp^3*-hybridized carbon, presenting properties such as high density, hardness and thermal conductivity, while the others has graphite-like *sp^2*-hybridized carbon. This latter type of compound is undesirable because it lacks the previous mentioned attributes. Then, the distinction between *sp^2*- and *sp^3*-hybridized carbon is of crucial importance in the characterization of *CN* films.

Several works have been published where X-ray photoelectron spectroscopy (*XPS*) is used as the key analytical technique to characterize *CN$_x$* films [5-14]. Although a complete satisfactory *XPS* assignation scheme for all the carbon and nitrogen peaks is lacking, there is a strong tendency to interpret the peaks as either "nitrogen bonded to *sp^2*-hybridized carbon" or "nitrogen bonded to *sp^3*-hybridized carbon". We assume that the origin of this type of interpretation comes from works where the hybridization differences for amorphous carbon films are determined from the shape of the *XPS C 1s* envelope, for example the work of Jackson [15]. However, this interpretation is, in some sense, contrary to the results of Belton and Schmieng [16], who concluded that, for diamond, amorphous carbon and graphite, regardless of hybridization state, all show the same *C 1s* binding energy in the *XPS* spectra. Besides, in other works, where the chemical state of nitrogen in nitrogen-containing polymer films was studied upon annealing, the reported binding energies are almost the same as those assigned to *N* bonded to *sp^3*-hybridized *C* [17]. Considering that in those polymer films it is very unlikely to find the formation of carbon *sp^3* bonds, and consistent with the reports of Belton and Schmieng, it is likely that the carbon hybridization state is not an *XPS* spectroscopically active for the case of *CN$_x$* films.

With the aim to resolve this conjecture, we prepared a series of films by pulsed laser deposition (*PLD*) and they were analyzed by *XPS*, Auger electron spectroscopy (*AES*), and electron energy loss spectroscopy (*EELS*). This deposition technique is known to grow high-density hard films [18], as diamond-like carbon (*DLC*) and related materials [19]. In order to incorporate nitrogen into the films, *N$_2$* gas was introduced in the reaction chamber and was ionized during the *PLD* process by gas-plume collisions. This method has proven to be useful in preparing nitride solid films with controllable stoichiometry [20-23]. Subsequently, films were annealed in the range from room temperature to *900^{o}C* in *50^{o}C* steps. This thermal treatment induces compositional and chemical changes in the deposited films. Soon afterwards, the *in situ* material evolution was recorded as a function of temperature by means of *XPS*, and the binding energies of carbon and nitrogen were carefully measured and compared.

2 Experimental procedure

2.1 Experimental setup

The experiments in this work were carried out on a modified laser ablation system, *Riber LDM-32*. This system has been described in more detail in a previous work [23]. Basically, the equipment consists of three

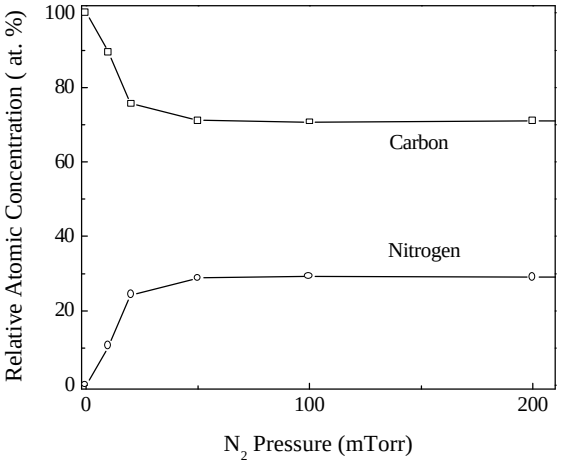

Figure 1. Relative atomic concentration determined by *XPS* as a function of nitrogen pressure.

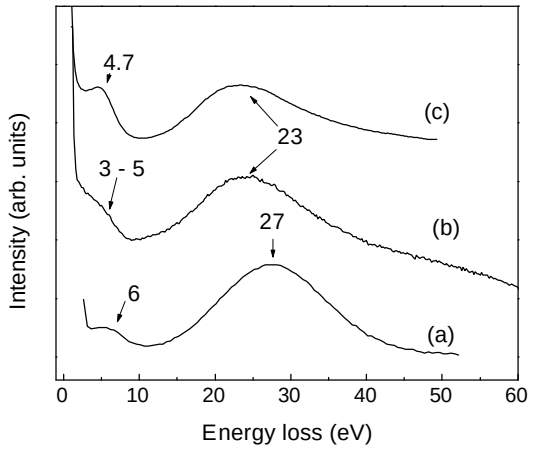

Figure 2. *EELS* spectra for (a) graphite ablation in high vacuum, (b) at *100 mTorr* of N_2 and (c) same sample as in (b) after annealing at *900 °C*.

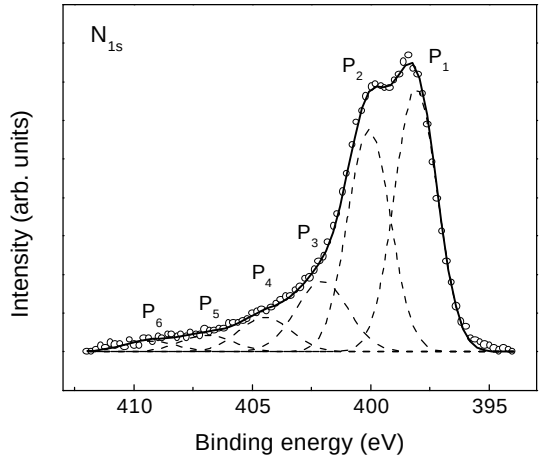

Figure 3. High resolution *XPS* of *N 1s* for a sample prepared at *100 mTorr* of N_2.

vacuum chambers: sample loading, film growth, and analysis. Each chamber is independently evacuated by an ion pump, and isolated by an ultra high vacuum (*UHV*) gate valve. The lowest attainable pressure is in the 10^{-10} *Torr* range for the growth and analysis chambers and in the 10^{-9} *Torr* range for the sample-loading chamber. A sample transfer system allows the rapid transport between the growth and analysis chamber. Ablation is accomplished by means of *a KrF* excimer laser (λ = *248 nm*, τ = *30 ns* full width at half maximum, *FWHM*) focused on the target at 50^o off from the surface normal.

The analysis chamber is equipped with an electron analyzer *Cameca MAC-3*, an e-gun and an X-Ray source to perform *XPS*, *AES* and *EELS* measurements.

XPS data were collected after exciting with the *Al* K_α line (*1486.6 eV*). The energy scale was previously calibrated using the reference binding energies of *Cu* $2p_{3/2}$ at *932.67 eV* and *Ag* $3d_{5/2}$ at *368.26 eV*. The *FWHM* obtained with this setup is *1.1 eV* measured on the *C 1s* transition of graphite. For *AES*, the primary energy was set to *3000 eV* and data acquisition performed at nominal resolution of *3 eV*. *EELS* data were collected using an incident e-beam of *1000 eV* and a resolution of *2 eV* measured on the *FWHM* of retrodispersed elastic electrons.

Gaseous films decomposition was monitored with a residual gas analyzer (*RGA*) *Balzers QMG-112*, located *3 cm* away from the sample holder.

2.2. Sample preparation and characterization

The *a-*CN_x films were grown on silicon substrates at room temperature by ablating a high purity graphite target in high vacuum and in the presence of molecular nitrogen under different pressures. Laser energy, number of pulses and pulse repetition rate were kept fixed at *800 mJ*, *10,000* and *10 Hz*, respectively. During the deposition process the pressure in the chamber was sustained by a turbomolecular pump and the main ionic pump was kept isolated by a gate valve. After completion of deposition process, the reaction chamber was evacuated to a pressure of 10^{-8} *Torr* in less than *3* minutes. At that point, the sample was translated to the adjacent analysis chamber. The effective time between the end of the growing process and the beginning of analysis is estimated to be less than five minutes. With this procedure, there is no incorporation of adventitious carbon in the films, and only traces of oxygen were detected.

The effect of temperature on these films was investigated by giving a thermal treatment to several samples. The substrate holder was resistively heated in front of the electron analyzer and the temperature kept constant by a closed loop controller. Surface film evolution and outgasing was recorded in 50°C steps from room temperature up to 900^oC by means of *XPS* and *RGA*, respectively.

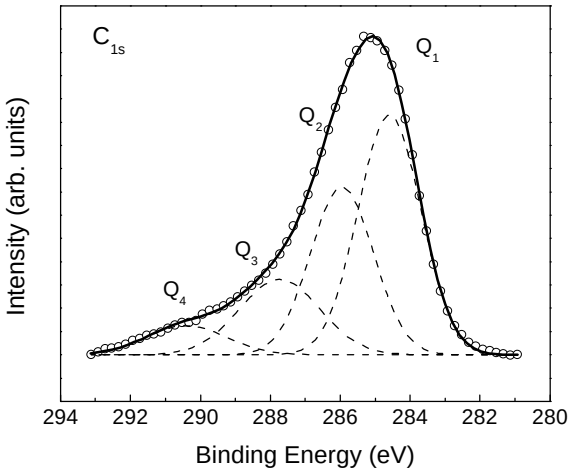

Figure 4. Same as in Figure 3 for transition *C 1s*.

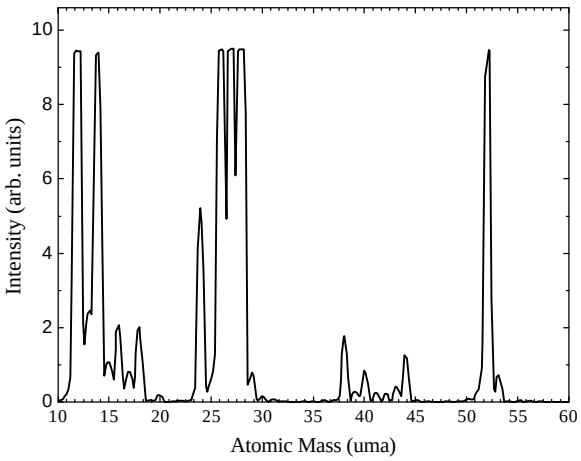

Figure 5. Ion Mass spectra of a sample grown at *100 mTorr* of N_2 held at *300* ^{O}C.

XPS data processing was performed as follows: first, a background subtraction using Tougaard's method [24]; then, in order to avoid biased solutions, a Gaussian fitting of carbon and nitrogen 1s levels was done in automatic mode using the *Origin 5.0* program [25], keeping the *FWHM* at *1.8 eV* for the main peaks. The number of peaks was fixed and their center proposed at an arbitrary energy. Finally, a quantification procedure was performed using reported sensitivity factors [26].

3. Experimental results

3.1 Nitrogen incorporation.

All the obtained *XPS* and *AES* spectra show that the prepared films contain only carbon, nitrogen and small traces of oxygen. Thus, we exclude from the subsequent discussion any *C-O* or *N-O* bonds. In Figure 1, the relative atomic concentration from *XPS* measurements of nitrogen and carbon as a function of nitrogen deposition pressure is presented. We observe a region of linear increment of the nitrogen signal, for films grown at low N_2 pressures, less than *20 mTorr*, while for pressures greater than *50 mTorr* a plateau is reached and no more nitrogen incorporation into the films is observed. This effect, although reported in other works at higher pressures, shows discrepancies that may be due to different laser conditions (fluence, repetition rate, wavelength, etc.) and target to substrate distance. The relative atomic concentration at this pressure range is about *70* and *30* percent for carbon and nitrogen, respectively. This corresponds to a stoichiometry of $CN_{0.4}$, in a good agreement with the usual values reported utilizing physical vapor deposition methods [27].

The deposition rate was also observed to be a function of gases pressure, i.e., the higher the pressure the lower the deposition rate. The highest deposition pressure is *500 mTorr*; above this pressure, no visible plasma or film deposition is perceived.

3.2. Electron energy loss spectroscopy

It has been proven *EELS* to be one of the most useful analytical tools for the diagnostic of different forms of carbon in thin films [16, 28]. In this work, *EELS* measurements were carried out in order to obtain the plasmon energy loss structure used as fingerprint for every sample. In Figure 2, films grown in vacuum (a), at *100 mTorr* of nitrogen (b), and at *100 mTorr* of nitrogen after annealing (c) are presented.

The films grown in vacuum, Figure 2(a), show the two main singularities of graphite, at an energy loss of about *27* and *6 eV*, corresponding to the $\sigma+\pi$ and $\pi-\pi^*$ electron plasma resonance, respectively [16]. For those films grown at *100 mTorr* of nitrogen, Figure 2(b), the $\sigma+\pi$ peak is shifted down to *23 eV* and the $\pi-\pi^*$ peak is ill defined, estimated in the *3* to *5 eV* region due to the wide background of inelastic backscattered electrons. The *EELS* spectrum obtained after annealing the same films grown at

Table 1.- Gaussian fit to Nitrogen *1s*.

Peak	Area	Center (eV)	Width (eV)	Height
P_1	39000	398.1	1.8	17290
P_2	34000	400.1	1.8	15070
P_3	10190	402.1	2.2	4520
P_4	5850	404.2	2.2	2600
P_5	3260	406.3	2.2	1440
P_6	2280	408.8	2.2	1010

Table 2. Gaussian fit to Carbon *1s*.

Peak	Area	Center (eV)	Width (eV)	Height
Q_1	62630	284.6	1.8	27760
Q_2	43630	286.1	1.8	19340
Q_3	16520	288.1	2.2	7320
Q_4	7980	290.4	2.2	3540

100 mTorr of nitrogen, in Figure 2(c), shows the principal electron energy loss at *23 eV*, similar to that of *100 mTorr* before annealing. However, the π–π* resonance is accentuated, showing a sharp feature at an energy of about *4.7 eV*.

3.3. X-Ray photoelectron spectroscopy

(a) *Gaussian Fitting*. For a detailed analysis of *XPS* spectra, the electronic 1s core levels of nitrogen and carbon were measured and numerically fitted to Gaussian functions. The fittings are similar to the reported values for *N 1s* and *C 1s*. They are presented in Figures 3 and 4, and their values in tables 1 and 2, respectively. The nitrogen *1s* region consists of two well-resolved binding energy configurations, P_1 at *398.1 eV* and P_2 at *400.1 eV*. For carbon *1s*, the observed broad peak, after fitting, shows two principal contributions to exist, Q_1 at *284.6 eV* and Q_2 at *286.1 eV*, as presented in Figure 4 and table 2. These features and their proportions are representative of our grown films. It is observed in Figures 3 and 4 that both peaks appear asymmetric towards the high binding energy side. This asymmetric tail is due to a process of inelastic scattering, strongly dominated by a π–π* resonance and detected by *EELS* with a characteristic energy of *4 eV* from the peak maximum. This feature in Figures 3 and 4 is associated with the so-called "shake-up" process and is found at *4 eV* to the high binding energy side from the main contributions, originating the noticed asymmetry. Numerical fitting of the tail generates first order P_3 and P_4 peaks, and second order P_5 and P_6 in the nitrogen region; and first order Q_3 and Q_4 in the carbon region.

3.4. Gas desorption mass spectroscopy

Ion mass spectra of a sample grown at *100 mTorr* of N_2 held at *300 °C* are shown in Figure 5. The features found on this sample are representative for every sample grown in this work, and only small differences in their relative intensities can be appreciated. The main peaks detected, their relative peak intensity, and possible assignment are given in Table 3.

Table 3. Classification analysis of products formed by the thermal decomposition of the films grown at *100 mTorr* of N_2. Only species with intensity >2% of maximum are tabulated.

Mass	Intensity	Chemical species
12	100	C
13	25	CH
14	90	N, CH_2
15	10	NH, CH_3
16	20	NH_2, CH_4, O
17	10	NH_3,OH
18	20	NH_4, H_2O
24	50	C_2
26	100	CN, H_2C_2
27	100	HCN,
28	100	N_2, H_2CN, CO
29	8	H_2C=NH
38	18	C_2N
39	3	HC_2N
40	8	CN_2, H_2C_2N
41	2	HCN_2, H_3C_2N
42	3	H_2CN_2, H_4C_2N
43	4	H_3C_2-NH_2
44	12	CO_2
52	100	C_2N_2
53	7	HC_2N_2

For this classification possible reactions with the residuals gasses proceed from analysis chamber (hydrogen and oxygen) has been considered, although not deliberately, hydrogen incorporation in the middle of the growth process can not be ruled out. Basically three different types of product gasses have been observed: Monomers and dimmers of the basic constituents (*C*, *N*, C_2, and N_2); cross products of them (*CN*, C_2N, CN_2, and C_2N_2); and reaction between the previous ones and hydrogen (CH_x, NH_x, H_xCN, H_xC_2N, H_xCN_2, HC_2N_2). From the presented spectra we observe that one of the most abundant masses is the one at *52 amu* and attributed to cyanogen. Considering that the sensitivity of cuadrupoles decrease with increasing mass number, the expected partial pressure for this component is much higher than the correspond to lower mass number and same intensity, so we believe that this is the principal constituent leaving the solid upon breakage of a large molecules embedded in the solid.

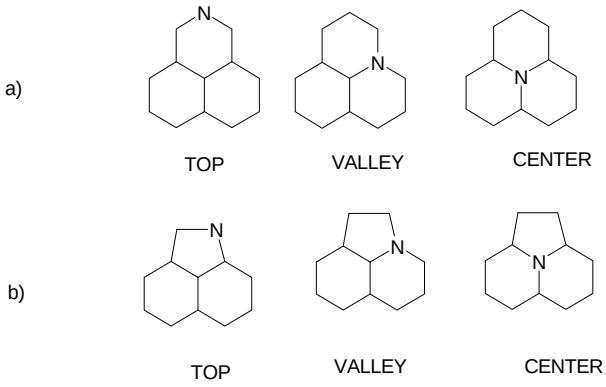

Figure 6. Pyridinic-like (a) and pyrrolic-like (b) nitrogen configurations with two and three carbon neighbors.

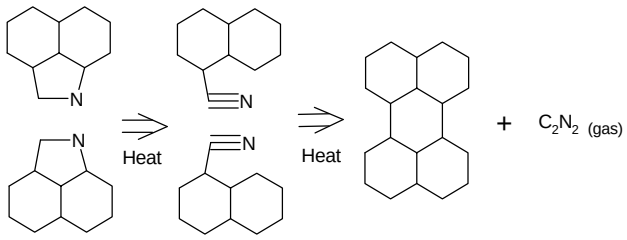

Figure 7. Proposed mechanism where two 'top position' nitrogen in pyrrolic cycles are used to sew up a graphene layer. C_2N_2 is released in the process.

4. Discussion

From the on-hand data, several observations can be made: the atomic concentration of nitrogen in the films decreases as a function of temperature; the nitrogen is leaving the solid in gaseous species, where C_2N_2 is the most abundant; and P_1 decreases more rapidly than P_2.

Even though in the films exists an important amount of chemical disorder, revealed by the broad *XPS* peaks, is helpful to simplify the analysis by linking the predominant nitrogen states, P_1 and P_2, with two particular chemical environments. Given the lower binding energy (*BE*) of the P_1 peak, it must be associated with a site where there are more available electrons than in the P_2 site. In aromatic-rings, the obtainable electrons are those that build up the π–system; then, the core-level-*BE* is an indirect measurement of the aromatic extent in which the nitrogen atoms have been fixed. The *BE* for six-member-ring (pyridine-like) is in the *398.3* to *399.34 eV* range, where the deviation is mainly due to the experimental uncertainty from choosing an adequate reference level [30]. The energy difference between the pyridinic and pyrrolic nitrogen, as determined from the reported data available in literature and revised extensively by J. Lahaye *et al.* [30], is in the *1.35-2.00 eV* range. Subsequently, it is likely the P_1 and P_2 sates of this study to be related to nitrogen in six- and five-member-rings, respectively.

In Figure 6, several heterocyclic configurations, pyrrolic- and pyridinic-like, are exposed. We can see that in the 'top-sites' the nitrogen atoms are prone to be removed. Figure 7 illustrates a proposed model of cycle-addition polymerization, where the top-nitrogen atoms are applied advantageous to sew up various contiguous carbon rings; C_2N_2 gas is generated in the course of actions. Given the chemical and structural disorder in the films, should exist many equivalent process that result in the release of N_2, $-C^{\circ}N$, C_xN, CN_x and all the other indexed masses.

On the other hand, the ternary varieties of nitrogen lying in sheltered locations, in valley and center sites, behave differently. In fact, the center-*N* is as stable as the surroundings are, remaining in carbon films heated up to *2200* ^{o}C [31-33] and unavailable to generate polymerization reactions. As a consequence, these nitrogen atoms are permanently stuck in the carbon matrix.

5. Conclusions

We have produced a material, which is similar to most reported CN_x films deposited using *PVD* methods. Although the binding energies reported for *C 1s* and *N 1s* agree well with reported values, we do not find any evidence that the material is composed of two phases. Moreover, in the *EELS* spectra, we don't find indication that carbon could be in a sp^3 configuration. On the contrary, the presence of the energy losses due to the π–π^* and σ+π plasmon at *6* and *23 eV* are a clear evidence of carbon in the more stable sp^2 configuration, with an electronic behavior similar to those of amorphous carbon network.

Two chemical states of nitrogen and carbon are present in these samples. *N 1s* peak at *398.1 eV* (P_1) is assigned to nitrogen in a strong electron-acceptor site, with three *C* neighbors in sp^2-configuration, and *N 1s* peak at *400.1 eV* (P_2), to nitrogen in a less-electron acceptor site, with two *C* neighbors in sp^2-configuration. Small N_{1s} contributions, peaks at *402.1 eV* (P_3) and *404.2 eV* (P_4) are labeled as resulting from an inelastic energy loss, the p-p^* electronic coupling process of the P_1 and P_2 emitted photoelectrons. Similarly, smaller peaks at *406.3 eV* (P_5) and *408.8 eV* (P_6) emanate from second order losses. Carbon peak at *284.6 eV* (Q_1) is attributed to *C* atoms surrounded by other C atoms only, like in graphite or diamond, while peak at *286.1 eV* (Q_2) is ascribed to *C* atoms bounded to one or more nitrogen neighbors in sp^2 coordination. Similarly to nitrogen, *C* peaks at *288.1 eV* (Q_3) and at *290.4 eV* (Q_4)

result from the energy loss due to p-p^* coupling from the two main peaks Q_1 and Q_2, respectively.

During thermal treatment, nitrogen leaves the film in a gaseous C_2N_2 compound and sub-products, as observed by thermal desorption mass spectroscopy.

The binding energy of *N 1s* in samples annealed at at high temperature indicates that *N* atoms are present as ternary nitrogen, or like in pyrrole, substitutionally doping carbon layers. This is in agreement with a model by Sjöström *et al.* [29] of a fullerene-like microstructure, where the cross-linking between two sp^2-hybridized CN_x layers are caused by buckling around pentagons. Thereafter, we give credence to that the improved mechanical properties of these *a*-CN_x films, reported in various works, is due to the mechanism proposed by Sjöström *et al*,. In this model the inclusion of pentagon ring (imidazole-like) in the structure of graphite produce the local shrinking and the twisting of graphite planes, leading to an amorphous solid with strong sp^2-hybridized bond in every direction. Thereafter, we disagree with the widespread predisposition that to forming a hard CN_x film, the sp^3-hybridization is essential.

Acknowledgements

The technical assistance of Israel Gradilla, Wencel de la Cruz, Francisco Ruiz, Eloisa Aparicio and Margot Sainz is gratefully appreciated. Financial support by Consejo Nacional de Ciencia y Tecnología (México) is also acknowledged.

References

[1] M. L. Cohen, Phys. Rev. B **32**, 7988 (1985).
[2] A. Y. Liu and M. L. Cohen, Phys. Rev. B 41, 10727 (1990).
[3] A. Reyes-Serrato, D. H. Galván and I. L. Garzón, Phys. Rev. B **52**, 6293 (1995).
[4] P. H. Fang, J. Mater. Sci. Lett. **14**, 536 (1995).
[5] S. Souto, M. Pickholz, M. C. dos Santos and F. Alvarez, Phys. Rev. B **57**, 2536 (1998).
[6] I. Gouzman, R. Brener and A. Hoffman, Thin Solid Films **253**, 90 (1994).
[7] Niklas Hellgren, Mats P. Johansson, Esteban Broitman, Lars Hultman and Jan-Eric Sundgren, Phys. Rev. B **59**, 5162 (1999).
[8] H. Sjöström, L. Hultman, J. –E Sundgren, S. V. Hainsworth, T. F. Page and G. S. A. M. Theunissen, J. Vac. Sci. Technol. A **14**, 56 (1996).
[9] D. Marton, K. J. Boyd, A. H. Al-Bayati, S. S. Todorov and J. W. Rabalais, Phys. Rev. Lett. **73**, 118 (1994).
[10] François Rossi, Bernard Andre, A. van Veen, P. E. Mijnarends, H. Schut, F. Labohm, Marie Paule Delplancke, Hugh Dunlop and Eric Anger, Thin Solid Films **253**, 85 (1994).
[11] J. Hartmann, P. Siemroth, B. Schultrich and B. Rauschenbach, J. Vac. Sci. Technol. A **15**, 2983 (1997).
[12] C. Ronning, H. Feldermann, R. Merk, H. Hofsass, P. Reinke and J.-U Thiele, Phys. Rev. B **58**, 2207 (1999).
[13] G. L. Chen, Y. Li, J. Lin, C. H. A. Huan and Y. P. Guo, Surf. Interface Anal. **28**, 245 (1999).
[14] M. A. Baker and P. Hammer, Surf. Interface Anal. **25**, 629 (1997).
[15] Stuart T. Jackson and Ralph G. Nuzzo, Appl. Surf. Sci. **90**, 195 (1995).
[16] David N. Belton and Steven J. Schmieg, J. Vac. Sci. Technol. A **8**, 2353 (1990).
[17] T. Nakahashi, H. Konno and M. Inagaki, Solid State Ionics **113-115**, 73 (1998).
[18] C. B. Collins and F. Davanloo, *Pulsed Láser Deposition of Thin Films*, edited by D. B. Chrisey and G. K. Hubler (Wiley, New York, 1994), Chap. 17.
[19] J. A. Martín-Gago, J. Fraxedas, S. Ferrer, and F. Comin, Surf. Sci. Lett. **260**, L17 (1992).
[20] E. C. Sámano, R. Machorro, G. Soto and L. Cota-Araiza, J. Appl. Phys. **84**, 5296 (1998).
[21] R. Machorro, E. C. Sámano, G. Soto and L. Cota, Appl. Surf. Sci. **127-129**, 564 (1998).
[22] G. Soto, E. C. Sámano, R. Machorro and L. Cota, J. Vac. Sci. Technol. A **16**, 1311 (1998).
[23] E. C. Sámano, R. Machorro, G. Soto and L. Cota-Araiza, Appl. Surf. Sci **127-129**, 1005 (1998).
[24] S. Tougaard, Surf. Interface Anal. **11**, 453 (1988).
[25] *Origin User Manual*, Published by Microcal Software Inc., Version 4.0, (1995).
[26] J. Moulder, W. Stickle, P. Sobol and K. Bomben, *Handbook of X-Ray Photoelectron Spectroscopy*, Edited by J. Chastain, Published by Perkin-Elmer Corporation, Eden Prairie (1992).
[27] Stephen Muhl and Juan Manuel Mendez, Diamond Relat. Mat. **8**, 1809 (1999).
[28] M. Avalos-Borja, G. A. Hirata, O. Contreras, X. G. Ning, A. Duarte-Moller and A. Barna, Diamond Relat. Mat. **5**, 1249 (1996).
[29] H. Sjöström, S. Stafström, M. Boman and J. –E. Sundgren, Phys. Rev. Lett. **75**, 1336 (1996).
[30] J. Lahaye, G. Nanse, Ph. Fioux, A. Bagreev, A. Broshnik, V. Strelko, Appl. Surf. Sci. **147**, 153 (1999).
[31] T. Nakahashi, H. Konno and M. Inagaki, Solid State Ionics **113-115**, 73 (1998).
[32] H. Konno, H. Oka, K. Shiba, H. Tachikawa, M. Inagaki, Carbon **37**, 887 (1999).
[33] H. Konno, T. Nakahashi, M. Inagaki, Carbon **35**, 669 (1997)..